

Selective Encryption of Medical Images

Aissa Belmeguenai, Lakhdar Grouche and Rafik Djemili

Laboratoire de Recherche en Electronique de Skikda, Université 20 Août 1955- Skikda,
BP 26 Route d'El-hadaeik, Skikda, Algeria

Keywords: Encryption by Region, Grain-128, Medical Images.

Abstract: The transfer of image in the digital world plays a very important role, their security is an important issue, and encryption is one of the ways to ensure security. Few applications like medical image security needs to secure only selected region of the image. This work proposes a selective encryption approach for medical images. The approach based on Grain-128 which provides the facilities of implementation of selective image encryption and decryption. Several tests are done in order to prove the approach performance including visual tests, key sensitivity, entropy analysis and correlation coefficient analysis.

1 INTRODUCTION

Sometimes the secure information is isolated in a one region or few regions of the image then encrypt only these regions, this allows us to gain considerable time. In this way, the encryption does not delay the process; instead it can be inserted as an integral part of the processing chain. In an application, when the selective encryption is adopted, the choice of regions to encrypt can be done in three ways which are: Manual: The regions are defined using the mouse as an electronic pen. Semi-automatic: In this case the regions are determined by program and always leave the user the possibility of a manual correction (Malet and al, 1988). For example, edge detection followed by a correction or improperly closed contours that overlap.

Automatic: When data parts are in the same coordinates location of the regions, these are predefined and the choice is made consistently. Sometimes the determinations of regions are programmed in first then the result of processing will be used to encrypt pilot regions. For example, for the following interest area that carries a particularity in the image. During an operation of Prenatal chromosome analysis and if the presence of a chromosomal abnormality of number, this is in the form of a trisomy 13 or trisomy 21 (Geneix and al, 1988), (Malet and al, 1989). However, when establishing the karyotype of the patient, the interest area (trisomy 13 or trisomy 21) from secret information and that they should be within the specialist doctor who has the sole authority to access and pronounce these results to the patient.

To keep this information secret, this paper describes an implementation of Grain-128 for selective encryption medical images. Several tests are done for proving the system performance including visual tests, correlation coefficient analysis, entropy analysis and key sensitivity.

2 GRAIN-128

In this section we give a brief description of Grain-128. The Grain-128 Keystream Generator was proposed by Hell, Johansson, Maximov, and Meier (M.Hell and W.Meier, 2006) as a variant of Grain-v1 (Canniere and Preneel, 2005), (C. Cid and Kurihara, 2009). The cipher consists of two 128-bit shift registers, one linear feedback (LFSR), one nonlinear feedback (NLFSR) and nonlinear Boolean functions h .

The feedback polynomial of the NLFSR has algebraic degree of two, and h has degree of three. The content of the LFSR is denoted by $u_i, u_{i+1}, \dots, u_{i+127}$ and the content of the NLFSR is denoted by $v_i, v_{i+1}, \dots, v_{i+127}$.

The LFSR is governed by the linear recurrence:

$$u_{i+128} = u_i \oplus u_{i+7} \oplus u_{i+38} \oplus u_{i+70} \oplus u_{i+81} \oplus u_{i+96}. \quad (1)$$

The NLFSR is governed by the nonlinear recurrence:

$$v_{i+128} = u_i \oplus v_i \oplus v_{i+26} \oplus v_{i+56} \oplus v_{i+91} \oplus v_{i+96} \oplus v_{i+3}v_{i+67} \oplus v_{i+11}b_{i+13} \oplus v_{i+17}v_{i+18} \oplus v_{i+27}v_{i+59} \oplus v_{i+40}v_{i+48} \oplus v_{i+61}v_{i+65} \oplus v_{i+68}v_{i+84}. \quad (2)$$

The contents of the LFSR and NLFSR represent the state of the Grain-128.

The combining function h of Grain-128 produces its output value based of the selected bits from the NLFSR and the LFSR as:

$$h(i) = u_{i+8}v_{i+1} \oplus u_{i+13}u_{i+20} \oplus v_{i+95}u_{i+42} \oplus u_{i+60}u_{i+79} \oplus v_{i+12}v_{i+95}u_{i+95}. \quad (3)$$

The output stream of the Grain-128 generates from the selected bits from the LFSR and NLFSR states and the output of h . it is computed as:

$$y(i) = \bigoplus_{j \in A} v_{i+j} \oplus h(i) \oplus u_{i+93}. \quad (4)$$

Where $A = \{2, 15, 36, 45, 64, 73, 89\}$.

3 SELECTIVE IMAGE ENCRYPTION

In this section, one is interested in the selective image encryption. In the selective image encryption, the encryption is not applied to entire data but it is applied to selected data only. Here the encryption process is applied only to the selected regions of interest leading to reduce the time for encryption see (N. S. Kulkarni and Gupta, 2008), (Z. Brahimi, 2008) and (Panduranga and al, 2013). Selection of interesting regions are done manually or automatically based on the application. To do this, we apply at the input of cryptosystem both informations (encrypted image and keystream generator) except that the keystream generator is controlled by encrypted areas.

Let f be the original image and g be binary image representing the regions to be encrypted, such that

$$g(i, j) = \begin{cases} 1 & \text{if } f(i, j) = \text{to encrypt} \\ 0 & \text{if otherwise} \end{cases} \quad (5)$$

At the reception the reverse operation is applied to extract the hidden information. Figure 1 shows the block diagram of selective image encryption process and figure 2 shows the block diagram of selective image decryption process.

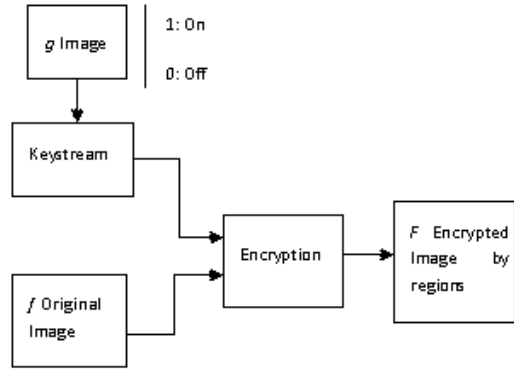


Figure 1: Block diagram of selective image encryption process.

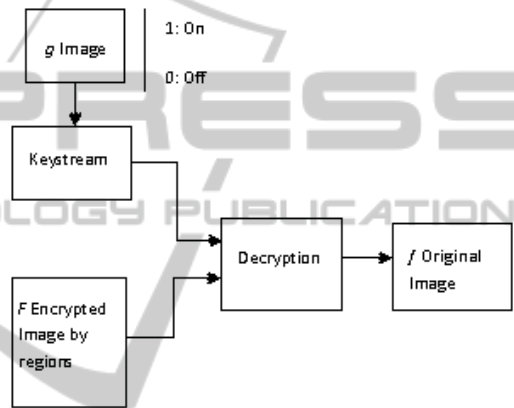


Figure 2: Block diagram of selective image decryption process.

4 PROPOSED SELECTIVE IMAGE ALGORITHM

The proposed selective image algorithm is using the Grain-128 keystream generator. Figure 3 depict the block diagram of the proposed approach. The flow charts of the encryption and decryption process are presented respectively in figures 4 and 5.

In a human Caryotype, the numbers of defects are usually trisomy 13 and trisomy 21 therefore observing three chromosomes in these boxes means that there is an anomaly of number, which means that the contents of these boxes must be within reach only of the doctor in charge. In addition, the doctor in charge wrote his final diagnosis in the observation part.

Since these three areas, boxes 13, 21 and the observation text constitute a confidential medical report then they are automatically hidden and accessible only by the doctor in charge. Thus, medical confidentiality is respected.

The individual steps of encryption and decryption

process are discussed in the following sub-sections. Let Caryotype (i.e. original image) of 391×300 pixels. Let R_1, R_2 and R_3 three regions of interest in Caryotype, respectively corresponding to boxes 13, 21 and the observation text. We denote by \oplus the sum modulo 2. By p, q and y we note respectively the digital selected regions, cipher digital selected regions and digital keystream.

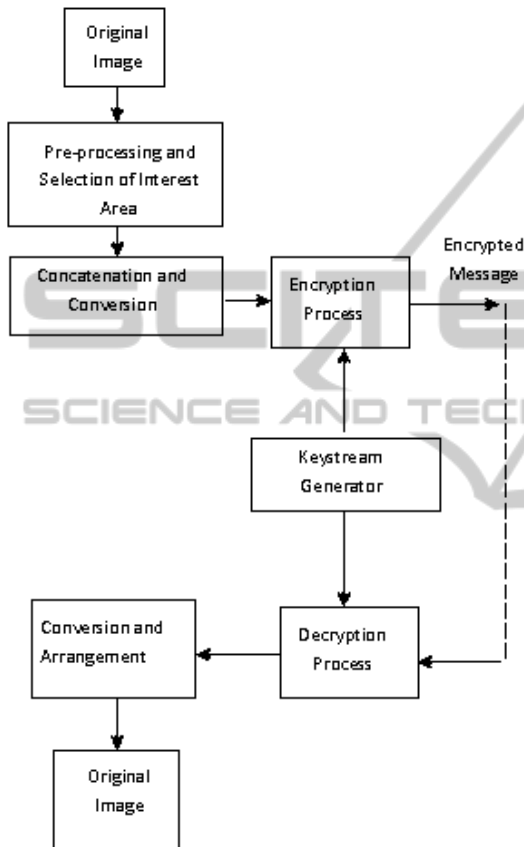


Figure 3: Block diagram of the proposed approach.

4.1 Pre-processing and Selection of Interest Area

At first, the Caryotype gray scale image is converted into a matrix of pixel values. Second, select R_1, R_2 and R_3 regions.

4.2 Concatenation and Conversion

Convert the region R_1, R_2 and R_3 into a one dimensional of decimal pixel values. This is then converted into a one dimensional binary sequence and stored it in p used for encryption process.

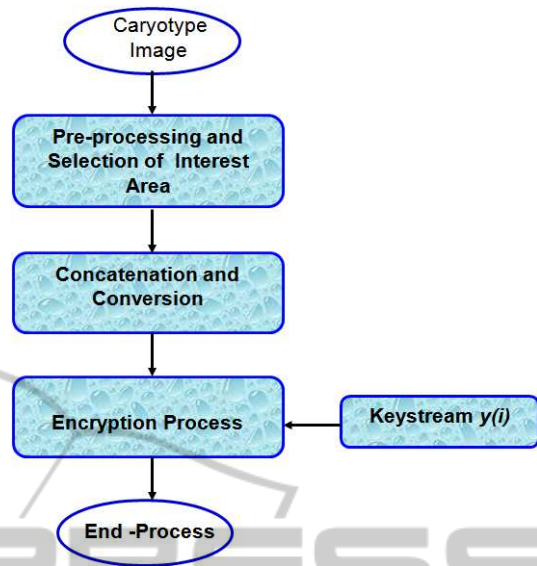


Figure 4: Flow chart of the encryption process.

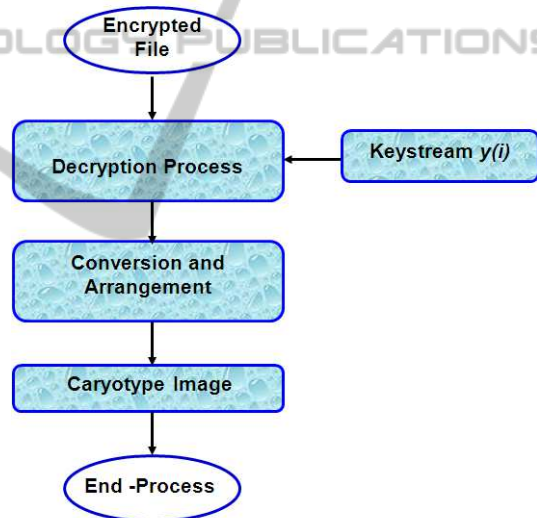


Figure 5: Flow chart of the decryption process.

4.3 Encryption Process

The encryption process work as follow:

- Load the digital selected regions p ;
- $N \leftarrow$ the length of p ;
- for $i = 1$ to N to make :
 - Generate the digital keystream y_i as it shows the keystream algorithm in section 4.6;
- End to make;
- for $i = 1$ to N to make:
 - Encrypt the digital selected regions p using relation

$$q(i) = p(i) \oplus y(i),$$

- End to make ;
- Sent the cipher digital selected regions q .

4.4 Decryption Process

The decryption process work as follow:

- Load the cipher digital selected regions q
- $N \leftarrow$ the length of q ;
- for $i = 1$ to N to make :
 - Generate the digital keystream y_i as it shows the keystream algorithm in section 4.6;
- End to make ;
- for $i = 1$ to N to make :
 - Decrypt the cipher digital selected regions using relation $p(i) = q(i) \oplus y(i)$
- End to make ;

4.5 Conversion and Arrangement

Convert the decrypted digital selected regions p into a one dimensional of decimal pixel values, then put each pixel in its place in the Caryotype image.

4.6 Keystream Algorithm

- Read N , length of the digital selected regions p ;
- Introduce the values of initialization of LFSR and NLFSR ;
- for $i = 1$ to $N + 127$ to make:
 - Generate binary sequences $u(i)$ and $v(i)$ respectively produced by LFSR and NLFSR as shown the equations 1 and 2;
- End to make.
- for $i = 1$ to N to make:
 - Generate the binary sequence $h(i)$ produced by the combining function h ;
 - Generate the output of keystream using the relation: $y(i) = \oplus_{j \in A} v_{i+j} \oplus h(i) \oplus u_{i+93}$.
- End to make.

5 SIMULATION AND RESULTS

In the simulation, three selected regions automatically R_1, R_2 and R_3 indicated in figures 6, 7 and 8 are used to validate the approach. Simulation was carried out using MATLAB V 7.5. By comparing the original regions and their corresponding encrypted regions in figures 6, 7 and 8, there is no visual information observed in the encrypted regions. Figure 9 show the visual testing of encryption and decryption for Caryotype.

In the experiments, the original regions and their corresponding encrypted regions and their histograms are shown in figures 6, 7 and 8. It is clear that the encrypted regions histograms are nearly uniformly distributed, and significantly different from the original regions histograms. So, the encrypted regions do not provide any clue to employ any statistical attack on

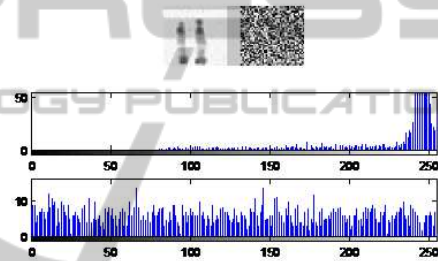


Figure 6: Experimental results for selected region R_1 : show the original region R_1 and its corresponding encrypted region and their histograms.

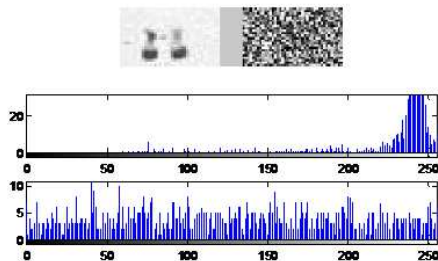


Figure 7: Experimental results for selected region R_2 : show the original region R_2 and its corresponding encrypted region and their histograms.

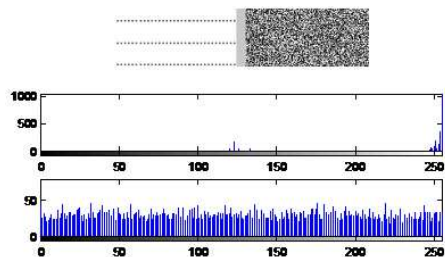


Figure 8: Experimental results for selected region R_3 : show the original region R_3 and its corresponding encrypted region and their histograms.

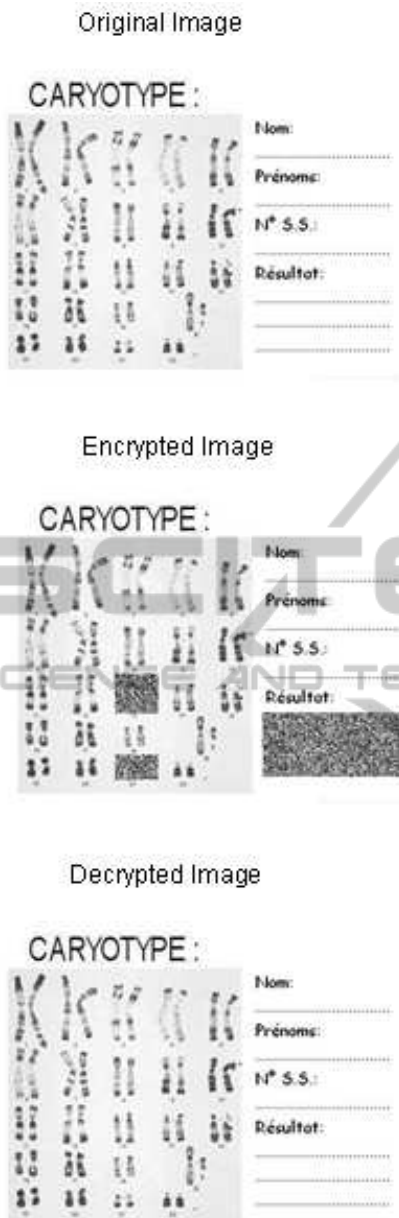


Figure 9: Visual testing of encryption and decryption for caryotype.

the proposed design, which makes statistical attacks difficult.

5.1 Correlation Coefficient Analysis

Table 1 and Table 2 show the correlation coefficient results. By Cor_1 , Cor_2 , Cor_3 , and Cor_4 we denote respectively correlation coefficient between original image and encrypted image, correlation coefficient between original image and decrypted image, correlation coefficient between encrypted image and de-

crypt image with wrong key and correlation coefficient between original image and decrypted image with wrong key.

It is observed that the values of Cor_1 , Cor_3 , and Cor_4 shown in the table 1 and table 2 are quite close to the value of zero, which implies that the original images and their encrypted images are totally different i.e. the encrypted image has no features and highly independent on the original image. It is also clear that the values of Cor_2 shown in the table 1 are equal to the value 1, which implies the encrypted images are the same as the original images.

Table 1: Correlation Coefficients Analysis.

Cases	Cor_1	Cor_2
Region 1	0.0100438	1.0000000
Region 2	0.0554183	1.0000000
Region 3	-0.0062774	1.0000000
Caryotype	0.0059980	1.0000000

Table 2: Correlation Coefficients Analysis.

Cases	Cor_3	Cor_4
Region 1	-0.0305526	0.0159771
Region 2	0.0688412	0.0102282
Region 3	-0.0058162	-0.0093714
Caryotype	-0.0024934	-0.0018975

5.2 Entropy Analysis

It is well known that the entropy $E(M)$ of a message source M can be calculated as:

$$E(M) = \sum_{i=0}^{T-1} P(M_i) \log_2 \frac{1}{P(M_i)}. \quad (6)$$

Where T Gray value of an input image (0-255), $P(M_i)$ represents the probability of symbol M_i and the entropy is expressed in bits. Let us suppose that the source emits 2^8 symbols with equal probability, i.e., $M = \{M_1, M_2, \dots, M_{2^8}\}$. Truly random source entropy is equal to 8.

Table 3 and table 4 show the entropy results. By E_1 , E_2 , E_3 , and E_4 we denote respectively entropy values: of original image, encrypted image, decrypted image and decrypted image with wrong key. The values of E_2 and E_4 presented in the table 3 and table 4 are very close to the theoretical value of 8. This means that information leakage in the encryption process is negligible and the encryption system is secure upon the entropy attack.

5.3 Key Sensitivity

A good cryptosystem should be sensitive to the secret

Table 3: Image Entropy.

Cases	E_1	E_2
Region 1	5.3746	7.8923
Region 2	5.3398	7.8101
Region 3	1.2416	7.9755
Caryotype	2.9176	7.9812

Table 4: Image Entropy.

Cases	E_3	E_4
Region 1	5.3746	7.8668
Region 2	5.3398	7.8128
Region 3	1.2416	7.9790
Caryotype	2.9176	7.9847

keys, which means change of a single bit in the secret key should produce a completely different encrypted image. The Grain-128 was tested to the keys sensitivity, we decrypt the encrypted regions illustrated by figures 6,7 and 8 with true key and, we decrypt the encrypted regions illustrated by figures 6,7 and 8 with wrong key (slightly different key). The results are given by figures 10 and 11. The values of Cor_3 and Cor_4 given in the table 2 are quite close to the value of zero, and the values of E_4 given in the table 4 are very close to the theoretical value of 8, which implies that the proposed cryptosystem is highly sensitive to the key.

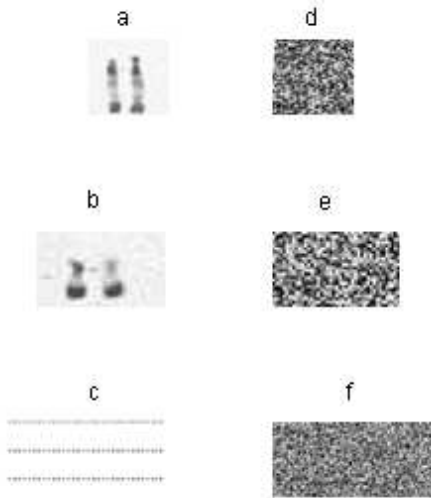


Figure 10: Sensitivity analysis: Frame (a), (b) and (c) respectively, show the decrypted regions with true key of the encrypted regions shown in figures 6,7 and 8. Frame (d), (e) and (f) respectively; show the decrypted regions with wrong key of the encrypted regions shown in figures 6,7 and 8.

6 CONCLUSIONS

In this Work, a selective image encryption algorithm

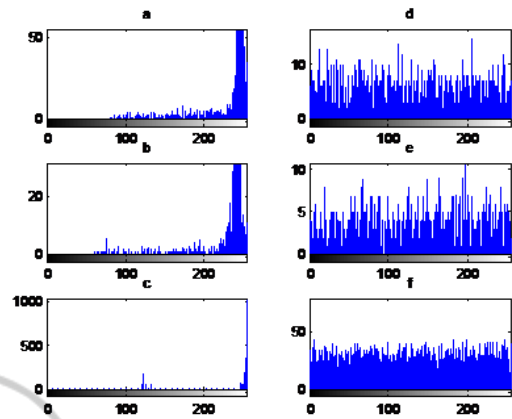


Figure 11: Sensitivity analysis: Frame (a), (b) and (c) respectively, show the histograms of decrypted selected regions with true key of the encrypted regions shown in figures 6,7 and 8. Frame (d), (e) and (f) respectively; show the histograms of decrypted regions with wrong key of the encrypted regions shown in figures 6,7 and 8.

for medical image using Grain-128 keystream generator was introduced. Simulations were carried out with three different selected regions. The visual test indicates that the encrypted regions was very different and no visual information can be deduced about the original region for all tested regions. This method is very simple, fast and easy to implement, as encryption and decryption selective image algorithm.

REFERENCES

C. Cid, S. K. and Kurihara, J. (2009). The rakaposhi stream cipher. In *Proceedings of the 11th international conference on Information and Communications Security, ICICS'09, Berlin, Heidelberg*. Springer-Verlag, pp. 32-46.

Canniere, C. D. and Preneel, B. (2005). Trivium a stream cipher construction inspired by block cipher design principles. In *eSTREAM, ECRYPT Stream Cipher Project, Report 2005/030 (2005-04-29)*. <http://www.ecrypt.eu.org/stream>.

Geneix, A. and al (1988). Image processing in human cytogenetics new steps toward quantification. In *Karyogram (U.S.A.)*. vol 14, p45-49,1988.

Malet, P. and al (1988). New cytogenetic techniques and medical applications. In *Sem Hop Paris*. 64, n23, 1576-1586,1988.

Malet, P. and al (1989). L'analyse chromosomique par traitement d'images aspects récents et perspectives. In *Annales de Génétiques*. vol 32, n3, p.164-16,1989.

M.Hell, T. and W.Meier (2006). A stream cipher proposal: Grain-128. In *IEEE International Symposium on Information Theory*. ISIT 2006.

N. S. Kulkarni, B. R. and Gupta, I. (2008). Selective encryp-

tion of multimedia images. In *NSC 2008*. December 17-19.

Panduranga, H. T. and al (2013). Selective image encryption for medical and satellite images. In *International Journal of Engineering and Technology (IJET)*. vol 5 No 1, 2013.

Z. Brahim, H. Bessalah, A. T. M. K. K. (2008). Selective encryption techniques of jpeg2000 codestream for medical images transmission. In *WSEAS Transactions on Circuits and Systems*. vol 7, July 2008.

